

Accepted version
Licence CC BY-NC-ND
Please cite as:

Rampazzi L., Andreotti A., Bressan M., Colombini M.P., Corti C., Cuzman O., d'Alessandro N., Liberatore L., Palombi L., Raimondi V., Sacchi B., Tiano P, Tonucci L., Vettori S., Zanardini E., Ranalli G. (2018), "An interdisciplinary approach to a knowledge-based restoration: The dark alteration on Matera Cathedral (Italy)", *Applied Surface Science*, Vol. 458, pp. 529–539, doi: <https://doi.org/10.1016/j.apsusc.2018.07.101>

1
2
3

An interdisciplinary approach to a knowledge-based restoration: The dark alteration on Matera Cathedral (Italy)

Applied Surface Science

Laura Rampazzi^{a,b*}, Alessia Andreotti^c, Mario Bressan^d, Maria Perla Colombini^c, Cristina Corti^a, Oana Cuzman^e, Nicola , Alessandro^d, Lolita Liberatore^f, Lorenzo Palumbo^g, Valentina Raimondi^h, Barbara Sacchi^e, Piero Tiano^e, Lucia Tonucciⁱ, Silvia Vettori^b, Elisabetta Zanardini^a, Giancarlo Ranalli^j

^aDepartment of Science and High Technology, University of Insubria, Via Valleggio 9, 22100 Como, Italy

^bInstitute for the Conservation and Valorization of Cultural Heritage - National Research Council of Italy (CNR-ICVBC), Via Cozzi 53, 20125 Milano, Italy.

^cDepartment of Chemistry and Industrial Chemistry, University of Pisa, Via Moruzzi 13, 56126 Pisa, Italy

^dDepartment of Engineering and Geology, University "G. d'Annunzio" of Chieti-Pescara, Via dei Vestini 31, 66100 Chieti, Italy

^eInstitute for the Conservation and Valorization of Cultural Heritage - National Research Council of Italy (CNR-ICVBC), Via Madonna del Piano 10, 50019 Sesto Fiorentino (FI), Italy.

^fDepartment of Economic Studies, University "G. d'Annunzio" of Chieti-Pescara, V.le della Pineta 4, 65127 Pescara, Italy

^gNello Carrara' Applied Physics Institute - National Research Council of Italy (IFAC-CNR), Via Madonna del Piano 10, 50019 Sesto Fiorentino (FI), Italy

^hDepartment of Philosophical, Educational and Economic Sciences, University "G. d'Annunzio" of Chieti-Pescara, Via dei Vestini 31, 66100 Chieti, Italy

ⁱDepartment of Bioscience and Territory, University of Molise, C. da Fonte Lappone, 86090 Pesche (IS), Italy.

*corresponding author

Laura Rampazzi, email address: laura.rampazzi@uninsubria.it

Abstract

An interdisciplinary analytical campaign was carried out on the exterior walls of the Santa Maria della Bruna and Sant'Eustachio Cathedral in Matera. Large areas of these walls have become darkened and the main objective was to evaluate the state of conservation of the stone material (a very porous, organogenic limestone called "Pietra di Matera"), and to suggest the best strategy for the current restoration. Several techniques were used in situ and ex situ-in laboratory analyses: X-ray diffraction, infrared spectroscopy, ion chromatography, pyrolysis/gas chromatography coupled with mass spectrometry, colour change measurements, laser-induced fluorescence together with biological techniques. Ex-situ and in situ cleaning tests were also carried out on the stone surface.

The results showed the presence of chlorophyll and bacteria on the surface, together with sulfation and calcium oxalate films as the main decay phenomena. In addition, the determination of saccharide and egg residues suggest both biological activity and past conservative treatments as the cause of oxalate films. Data obtained from the analyses proved to be very useful for the conservation work; a complex plan of restoration was adopted, including both traditional and innovative techniques (such as biocleaning, bacterial-gel and a laser system) together with a final evaluation of several protective methods.

Key words

Tuff dark alteration, FTIR, LIF, Py-GC-MS, calcium oxalate film, biocleaning

Highlights

- The dark alteration was identified as calcium oxalate film
- Cyanobacteria, bacilli, heterotrophic and cocci type bacteria were identified

- Films are probably due to both biological activity and residues of past treatments
- Results of the campaign suggested the best chemical cleaning method
- The most effective protective agent was identified

Introduction

Matera Cathedral was built in Romanesque-Apulian style in 12th century in the old part of Matera (Italy), called “*I Sassi*”, that is an agglomeration of almost completely abandoned dwellings made of the local rock (tuff) of the Gravina torrent valley. Matera lies at the western edge of an area called *Parco Archeologico Storico Naturale delle Chiese Rupestri del Materano*, which is listed in UNESCO World Heritage sites.

The exterior walls of the Cathedral, made of the local calcareous tuff, have shown a wide dark alteration in the lower part of the structure (up to 6-8 meters) since at least the beginning of 20th century (Figure 1). The phenomenon was worrying, for the serious aesthetic damage to one of the most important landmarks of Matera. No historical information could explain the alteration, for example whether it has originated from past surface protection treatments. The research on the sources of the dark alterations was no easy up today because it did not seem to relate only to a superficial film or to an unknown phenomenon affecting the stone inside.

Conservation work undertaken from 2014 to 2016 was a unique opportunity to examine the state of conservation of the surfaces, to provide new insights into the dark alteration and to propose a cleaning strategy. The characterization of the stone surfaces of monuments was very important in order to identify the decay phenomena, which could be both biological and chemical, and indirectly provides information on the conservation history of the building [1].

An interdisciplinary team of experts in Conservation Science-biologists, chemists, geologists, and physicists-thus was created in 2015 for planning an extensive analytical campaign, composed both by *on-site* and *ex situ* analyses and cleaning tests (Table 1). A multi-technique approach prior to a conservation work is fundamental to consider and study the decay phenomena from various points of view, being this strategy a good practice also for the knowledge of the artistic techniques, provenance of materials, testing of restoration materials as evident in the recent literature [2–8]. In this study, the importance of the monument and the age of the dark alteration has required a working group with complementary and multiple expertise and skill, to consider as many aspects as possible and to come up with a proposal with the effective cleaning method.

During the first step (Table 1), a non-invasive monitoring of the surfaces, based on the use of fluorescence (LIF) and colorimetric investigations, was planned in order to map the presence of biodecay phenomena and to verify a selection of cleaning methods, including a biocleaning treatment. The LIF technique is based on the induction of the fluorescence of the surface of interest by means of a laser source emitting at a suitable wavelength. The signal backscattered by the irradiated surface is collected and detected using a spectrometer. The experimental setup for the analyses of the Cathedral of Matera was tailored for recording the fluorescence signals both of the stone material and of photosynthetic pigments typical of photoautotrophic organisms. The results may enlighten the presence of chlorophyll, which is a clue of a biological patina colonizing the surface.

The sampling of small fragments from the most representative altered areas was performed as well and the samples were characterized by traditional and innovative techniques, seeking for the features of the on-going decay, that are inorganic and organic components and microorganisms. In particular, X-ray diffraction (XRD) and optical microscopy (OM) were used for pointing out the mineralogical phases and evaluating the stratigraphy of the mortar, Fourier transform infrared spectroscopy (FTIR) for the identification of inorganic compounds, ion chromatography (IC) for the quantification of water-soluble salts, pyrolysis-gas-chromatography coupled with mass spectrometry (Py-GC-MS) for characterizing the organic fraction. The results guided the practices of removal of the decay, depending on the presence of bio-colonisation or insoluble compounds.

108 The cleaning strategy was studied in Step 2 (Table 1), evaluating bio- and chemical- methods both in
 109 ex situ tests on stone specimens and in in situ experiments, also considering ablation by laser. The in
 110 situ tests were monitored by evaluating the colour changes of the surface. In addition, various
 111 protective agents were tested and applied in situ, evaluating the results with non-invasive reflectance
 112 FT-IR and Py- GC-MS on micro-fragments.

113 The results from Steps 1 and 2 were used to define the best cleaning method and the best protective
 114 agent. This was carried out during Step 3, and was completed in 2017. The data concerning the choice
 115 and monitoring of the protective agents are discussed in detail elsewhere [9]. Only some aspects are
 116 mentioned in the conclusions of this paper, in order to emphasize the importance of a preliminary
 117 analytical campaign in protecting the stone surface.

118
 119 **Table 1**
 120 Description of the analytical campaign
 121

Wall surface	Phases and site	Methodology	Instruments/Methods/Materials
Step 1 Analyses	Sampling	Manual scalpel and cuts Physical	
	Analyses <i>on-site</i>	Optical	LIF, Colorimetric analysis, OM observation
	Analyses <i>ex situ</i>	Chemical Biological	FTIR, XRD, IC, Py-GC-MS Microbial viable counts, ATP assay
Step 2 Cleaning	Test <i>ex situ</i>	Chemical cleaning	H ₂ O ₂ , UV, Oxone ®, TiO ₂
		Biocleaning	Impact biogel
	Test <i>on-site</i>	Physico-Mechanical	Micro-laser
		Chemical	H ₂ O ₂ , AB57 Impact - poultice
		Biocleaning	Impact biogel
	Protection	Chemical	FTIR, Py-GC-MS
	Monitoring	Physical Optical	Water absorption Colorimetric analysis
Step 3 Cleaning	At <i>on-site</i> full scale	Chemical cleaning	Impact - poultice
		Physico-Mechanical	Micro-laser
	Restoration	Chemical	Final protective agents

122
 123



125 Figure 1 Exterior of the Matera Cathedral facade (Matera, Italy) with the evident dark alteration-in the lower part of the
126 structure (up to 6-8 meters) (above). The provenance of the samples (bottom).
127

128
129
130
131
132

133
134
135
136
137
138
139
140
141
142
143
144
145
146
147
148
149

2. The experimental

2.1 Step 1

2.1.1 Sampling

Eight samples (C1-C7, OG) of “Pietra di Matera” and mortar (C4 sample) were taken from the stone surfaces of the southern wall and from the façade, both as powder and fragments scraped off the surface using a scalpel (Table 2). Selective sampling of C4 and C6 sample was carried out by a micro-lancet under an optical microscope, in order to analyse the three and two layers of the stratigraphy, respectively. The samples of powders for the biological analyses (B1-B4) were scraped off the surface with a sterile chisel (Table 2).

Figure 1 shows the points of sampling. The areas chosen for *on-site* analyses are shown too.

Table 2
Description of the samples

Sample label	Provenance	Description
C1	Southern wall	dark area, powder
C2		ochre area, powder
C3		ochre area, fragment
C4	Façade	ochre area, fragment of mortar
C5		dark area, powder
C6		ochre area, fragment
C7		ochre area, fragment
B1	Southern wall	powder (close to sample C1)
B2		powder (close to sample C2)
B3		powder (close to sample C3)
B4	Façade	powder (close to sample C4)
OG		ochre painted area, fragment

150
151
152
153
154
155
156
157

2.1.1.1 “Pietra di Matera” specimens

A noble tuff block (36 x 22 x 25 cm, 40 kg) was sampled at 1,5 meters from the ground on the left external facade wall of Cathedral and removed (Figure 2). It was cut horizontally by dry mechanical saw into thinner specimen blocks (36 x 22 x 3.5 cm, each; the external ones with the noble surface; the inners as artificial tests) and used for *ex situ* chemical and biocleaning treatments. The hole created by removal was filled by another block of a vile tuff of the same measurements [9].



158
159
160
161

Figure 2. *On-site* sampling of ancient tuff sandstone at left side of Matera Cathedral.

Laser-Induced Fluorescence (LIF)

162 The LIF technique used to acquire the measurements is based on the induction of the fluorescence of
163 the surface of interest by means of a laser source emitting at a suitable wavelength. The signal
164 backscattered by the irradiated surface is collected and detected using a spectrometer.

165 The instrumentation used to acquire the LIF spectra was an in-house developed fiber-optics-coupled
166 portable LIF spectrometer powered by batteries. The laser source was chosen to optimise the
167 induction of the fluorescence in the photosynthetic pigments, and particularly chlorophyll. The
168 fluorescence signal was detected in the spectral range between 450 nm and 930 nm with a spectral
169 sampling interval of approximately 0.5 nm. The optical and mechanical configuration of the handheld
170 measuring head is configured to acquire the fluorescence signal on circular area of about 5 mm in
171 diameter.

172 173 *Optical Microscopy (OM)*

174 *Reflected light microscopy* Polished cross-sections were obtained from fragments of some collected
175 samples. A Nikon Eclipse E600 Microscope, connected to a high-resolution digital camera and
176 controlled by NIS Elements Software for image analyses, was used.

177 *Transmitted light microscopy* Petrographic observation on a thin section of 30 μm thickness was
178 performed to obtain the main textural-compositional parameters of the C4 plaster sample. An optical
179 transmitted light polarized microscope, Zeiss AxioScope A.1, with parallel and cross nicols, with
180 2.5X, 5X and 10X of magnification was used. The acquired images were processed with Axiovision
181 software.

182 183 *Fourier transform infrared spectroscopy (FTIR)*

184 The samples scraped off the paint layer were analyzed as KBr (Sigma-Aldrich FTIR Grade) pellets
185 by a FTIR spectrophotometer BioRad Excalibur Series FTS 3000, DTGS detector, in the transmission
186 mode (400 to 4000 cm^{-1} , 4 cm^{-1} resolution, 16 scans). The samples C5 and C7 were analysed by means
187 of a portable Bruker Optics ALPHA FTIR Spectrometer equipped with SiC Globar source and DTGS
188 detector, collecting 24 scans in ATR mode, with 4 cm^{-1} resolution in the 4000-400 cm^{-1} range. The
189 collected spectra were elaborated with an OPUS 7.2 Software.

190 Non-invasive FTIR measurements were carried out with an Alpha Bruker FTIR portable
191 spectrophotometer in reflection mode for contactless measurements and a DTGS detector. Spectra
192 were collected between 7000 and 400 cm^{-1} with 4 cm^{-1} resolution and 128 scans on a 4mm-diameter
193 area. The average working distance from the surface was about 1 cm.

194 195 *Ion Chromatography (IC)*

196 Ion chromatography analyses were performed with a Dionex ICS-1000 instrument, equipped with a
197 suppressed conductivity detector. For cation analyses, an IonPac® CS12 4x250 mm analytical
198 column - which is specifically conceived for the analysis of alkali metals, alkaline earth metals and
199 ammonium - and an IonPac® CG12 4x50 mm Guard Column. The eluent was methane sulfonic acid
200 20 mM and the suppressor was a cation self-generating suppressor 300x4mm (CSRS® 300). For
201 anion analyses, an IonPac® AS 4A 4x250 mm analytical column and an IonPac® AG 4A 4x50 mm
202 guard column were used. The eluent was an aqueous solution of Na_2CO_3 (1.8mM) and NaHCO_3
203 (1.7mM) and the suppressor was an anion self-generating suppressor 300x4mm (ASRS® 300). ICS-
204 1000 operation is remote controlled by Chromeleon Software (version 6.7 SP1) that also provides
205 data acquisition and data processing functions. For the chromatographic analyses, a given amount of
206 water was added to a weighted amount of the sample. The solution was then stirred for 24 hours,
207 decanted and filtered with hydrophilic PTFE filters (pore size 0.45 μm).

208 209 *Pyrolysis Gas Chromatography Mass Spectrometry (Py-GC-MS)*

210 A pyrolyser operating in constant temperature mode (multi-shot pyrolyzer® EGA/PY-3030D
211 (Frontier Lab), connected to a split/splitless injector of a 6890N Network GC System gas
212 chromatograph (Agilent Technologies, Palo Alto, CA, USA), coupled with a 5973 Mass Selective

213 Detector (Agilent Technologies, Palo Alto, CA, USA) single quadrupole mass spectrometer, was
214 used. The mass spectrometer was operating in the electron impact (EI) positive mode (70 eV).
215 The pyrolysis conditions employed for the analysis of the samples were: furnace temperature 500°C,
216 interface temperature 300°C. In the pyrolysis cup, 2 µl of Hexamethyldisilazane (HMDS) was added
217 to a few micrograms of each sample. The gas chromatograph was equipped with a HP-5MS fused
218 silica capillary column and the chromatographic parameters are reported in literature [10,11].
219

220 *X Ray Diffraction (XRD)*

221 In order to identify the mineralogical composition, XRD analysis was performed. A PANalytical
222 X'Pert PRO X-ray diffractometer with Cu anticathode ($\lambda = 1.54 \text{ \AA}$) was used, under the following
223 conditions: current intensity of 30 mA, voltage 40 kV explored 2Θ range between $3^\circ - 70^\circ$, step size
224 0.02° , time to step 50 s and scan speed of $0.04^\circ/\text{s}$. The instrument was equipped with X'Celerator
225 multirevelatory and High Score data acquisition and interpretation software.

226

227 *Biological analyses*

228 The samples have been observed in transmitted and UV light with an optical microscope (Nikon
229 Eclipse E600 with an UV-2A filter). A small aliquote of the collected powder (10 mg) was sown on
230 three different nutrient media: potato dextrose agar for micromycetes (PDA, Difco), (plate count agar,
231 for heterotrophs such fungi and bacteria (PCA, Difco), and BG₁₁M liquid medium for algae and
232 cyanobacteria [12]. Another nutrient media, nutrient agar (NA, Difco) was used for isolating bacteria
233 developed on PCA. The isolated bacterial strains were gram-stained and observed in transmission
234 mode, while unstained colonies were observed using the UV-light.
235

236 **2.2 Step 2**

237 *Microorganism, media and ex situ biological test*

238 On the basis of previous results, *P. stutzeri* strain A29 (DISTAM-DISTAAM Strains Collections,
239 University of Milan - University of Molise, Italy), was used for the biocleaning processes [13,14].
240 In order to optimize growth conditions for the cells to be applied to the altered stone surface, an
241 assessment was made of biodegradation activity: the strain was incubated at 28°C for 24-36 hours,
242 on mineral medium M9 and on the same medium supplemented by organic substances, as linseed oil
243 or egg (CTS srl, Altavilla Vicentina, Italy) at 0.5% v/v and 0.5% w/v, respectively.

244 Suspensions containing exponentially-growing bacteria, approximately 10^8 CFU ml^{-1} were obtained
245 by inoculating 10 ml of an overnight broth-culture into 1,000 ml of fresh broth medium (in a flask of
246 3,000 ml total volume) and incubating it in a shaker (200 rpm) for 24 hours at 28°C. The cells were
247 centrifuged at 7,000 g for 10 minutes at 4°C, washed twice with phosphate-buffered saline solution,
248 and re-suspended in sterile distilled water, at pH 6.9; the final cell concentration was above 10^8 cells
249 ml^{-1} , corresponding to an O.D._{560 nm} of about 1.6; pH was about 7.0 and the solution conductivity was
250 about $947,1 \mu\text{s cm}^{-1}$; the cells were stored at 4 °C before bio-applications.

251 In these biocleaning tests laponite was adopted as delivery system instead of the agar gel that needs
252 higher temperature before solidification. The choice of this delivery system was made according to
253 the requirements and limitations of each work of art [15]. In duplicate, laponite gel (control) and
254 laponite gel including bacteria (laponite biogel, at 9.0 % w/v in the suspension bacterial cells) were
255 employed. A 0.8 - 1.0 cm thick continuous layer of *P. stutzeri* A29 cells entrapped in the laponite
256 delivery system was applied onto the *ex situ* noble tuff surface using a sterile spatula. The entire piece
257 was uncovered with any layer plastic film in order to favour the aerobic conditions; the application
258 times were optimised and ranged 12 -24 hours with a room temperature of $25^\circ\text{C} \pm 2^\circ\text{C}$.
259

260 *Ex situ chemical tests*

261 In order to evaluate the cleaning of the altered brownish area, advanced oxidation processes (AOPs)
262 were considered. They are designed to produce hydroxyl radicals that are highly efficient to destroy

263 organic compounds residues. Therefore, AOP constitute a crucial technology for the degradation of
264 non-easily removable organic compounds. AOP combine, for example, ozone (O₃), ultraviolet
265 irradiation (UV), hydrogen peroxide (H₂O₂) and/or (photo)catalysts (e.g., Fe ions, TiO₂,
266 polyoxometalates) to offer a powerful solution for the decrease or the removal of residual [16–20].
267 For example, the entire surface of a noble tuff specimen was split out in vertical and horizontal
268 regions. Several oxidation reagents were tested on the stone surface: H₂O₂, commercial Oxone®,
269 TiO₂, UV light irradiation, H₂O₂+UV light and TiO₂+UV light. H₂O₂ was used at 35%; Oxone was
270 dissolved in water solution (0.1 M concentration of active oxygen as KHSO₅). Mixture of TiO₂ was
271 obtained sonicating 0.75 g anatase and 0.25 g rutile in 10 mL deionized water for 10 min.
272 For photochemical reactions, a photochemical multiray apparatus (Helios Italquartz; Milano, Italy)
273 was used, which contained 10 UV lamps of 15 W power each that emitted light around 254 nm. All
274 chemicals are purchased from Sigma Aldrich and used as such.

275 *On-site chemical and biological treatments*

276 *On-site* chemical cleaning tests on the outer wall of Matera Cathedral were carried out adopting two
277 different cleaning agent; H₂O₂ at 35% and AB57 agent (Istituto Centrale del Restauro, ICR Rome)
278 The AB57 include inorganic salts (ammonium bicarbonate, sodium bicarbonate, EDTA disodium
279 salt, quaternary ammonium salt, carboxymethyl cellulose) in aqueous solutions with other reagents
280 and inert materials for the preparation of cleaning mixtures and poultice to be applied to stone surfaces
281 and frescoes (CTS srl, Altavilla Vicentina, Italy).

282 The area selected for the *on-site* bioapplication was part of the external wall of the right side of the
283 Cathedral and was about two square meters (Figure 3), distinguish area with same size (25x40 cm)
284 as follows: i) Laponite delivery system +enriched with *P. stutzeri* A29 cells (biogel); ii) Laponite
285 carrier alone as a control using only the delivery system without bacterial cells (control 1, gel).
286 Finally, the second control test of an untreated area, no carrier, was used as comparison. For each
287 area tested about 0.3 kg of the delivery system, which had been stored in sterile plastic box, was used;
288 the application and distribution was facilitated by sterile flat plastic spatulas, which made it possible
289 to apply thin layer gel averaging 0.5 cm in depth.

290 Representative areas from around 25 cm² to around 1,000 cm² were selected and bio-application tests
291 were performed as following:

- 292 i) Japanese paper, 9.0 g/m², natural, white, un-buffered (Klug Conservation, Walter GmbH & Co.
293 KG., Immenstatd, Germany) was applied in respect to the artwork.
- 294 ii) Laponite and laponite-bacterial gels without or with suspension of *P. stutzeri* viable cells (biogel),
295 respectively, were obtained by manually mixing components with a plastic spatula, for 5 min;
- 296 iii) The delivery systems (laponite-gel or laponite-bacteria gel, biogel) were stored at 4°C or
297 immediately applied to the selected areas;
- 298 iv) Japanese paper, sterile water and the delivery system as negative controls (only laponite gel) were
299 performed on each artwork. No other facilities were adopted (as plastic net or a plastic film to reduce
300 evaporation of water).

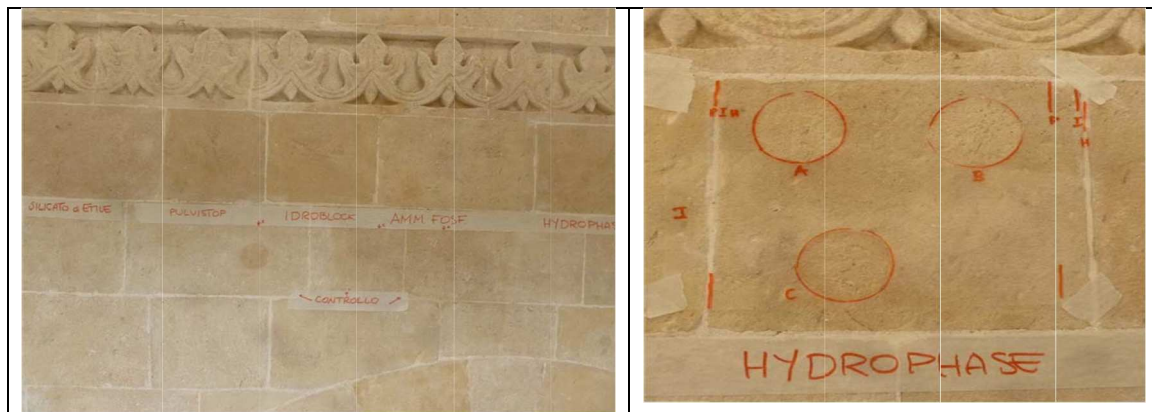
301 At different lengths of time from the bioapplication of viable bacterial cells (after 12 and 24 hours
302 respectively), the biogel layers were removed by soft brush from the surface of the stone wall and the
303 areas were subjected to three gentle manual washes using a soft sponge soaked in distilled water.
304 Samples from all the cleaned and control areas were removed after contact, and sample stone were
305 collected for chemical and microbiological analysis. Three replicates (30 x 20 cm) were made for all
306 biocleaning and control tests. During bioapplication, outdoor environmental temperature was
307 recorded.

308 *Physical cleaning (laser technology)*

309 A laser group with integrated cooling system and microprocessor control panel for the laser beam
310 frequency and power - a laser hand-piece with a 3 m optical fiber, easy to-use and particularly suitable
311 for *on-site* works was adopted (mod LIGHT II Laser, CTS srl, Altavilla Vicentina, IT).

314

315



316 Figure 3. View of tuff stone area selected for the *on-site* treatment at Matera Cathedral (left). A particular of musk adopted
317 on the wall to facilitate the re-position both of the colorimetric probe and the contact sponge (right).
318

318

319 **2.2.2 Monitoring**

320 *Colour measurements*

321 Colour measurements (Miniscan with light D65; Hunter Lab, Bergamo, Italy, and a portable Minolta,
322 mod. Chromameter CR200), were adopted to evaluate any chromatic changes on the paint of the
323 biocleaned surface on several previously selected areas, over the short and medium term. The
324 chromatic coordinates L* (brightness), a* (difference between green and red), and b* (difference
325 between yellow and blue) of the wall surfaces were determined according to the CIE L*a*b* standard
326 colour system [9,21].

327 For each ancient tuff stone samples adopted both at *ex situ* lab trials and on the wall of the Cathedral
328 as before described, several points of analysis (3-5) and (6-9), respectively, were selected; the
329 instrument was set to automatically give the average value of the colorimetric coordinates (L*, a*,
330 and b*) of the replicates (n. 3) measurements of each point, on each circle area selected. (Figure 3).
331 The results of the chromatic change (ΔE^*) was calculated by means of the following equation:

332

$$333 (\Delta E^*) = \sqrt{[(\Delta L^*)^2 + (\Delta a^*)^2 + (\Delta b^*)^2]}$$

334

335 Finally, for each sample the (ΔE) values were mediated to obtain a single value and the standard
336 deviation. The measurements were carried out on the same points, before and after the biological and
337 chemical tests, by using an adequate mask.

338

339 *Water uptake test (capillarity water adsorption)*

340 To estimate a water uptake coefficient on the tuff surface of selected area, the contact sponge method,
341 a non-destructive *on-site* methodology, was used [22]. The UNI Normal procedure requires to use a
342 sponge with known density (Spontex1 type Calypso) soaked in water, weighed, placed on surface of
343 the material for 1 minute, then weighed again [23]. Moreover, we adopted adequate paper disks
344 (circular surface about 24 cm², diam. 6.0 cm) for the measurements, before and after the application
345 of several treatment of cleaning and/or selected protective materials; for each treatment, mean of 3
346 replicated values were calculated (Figure 4).

347

348 **3. Results and Discussion**

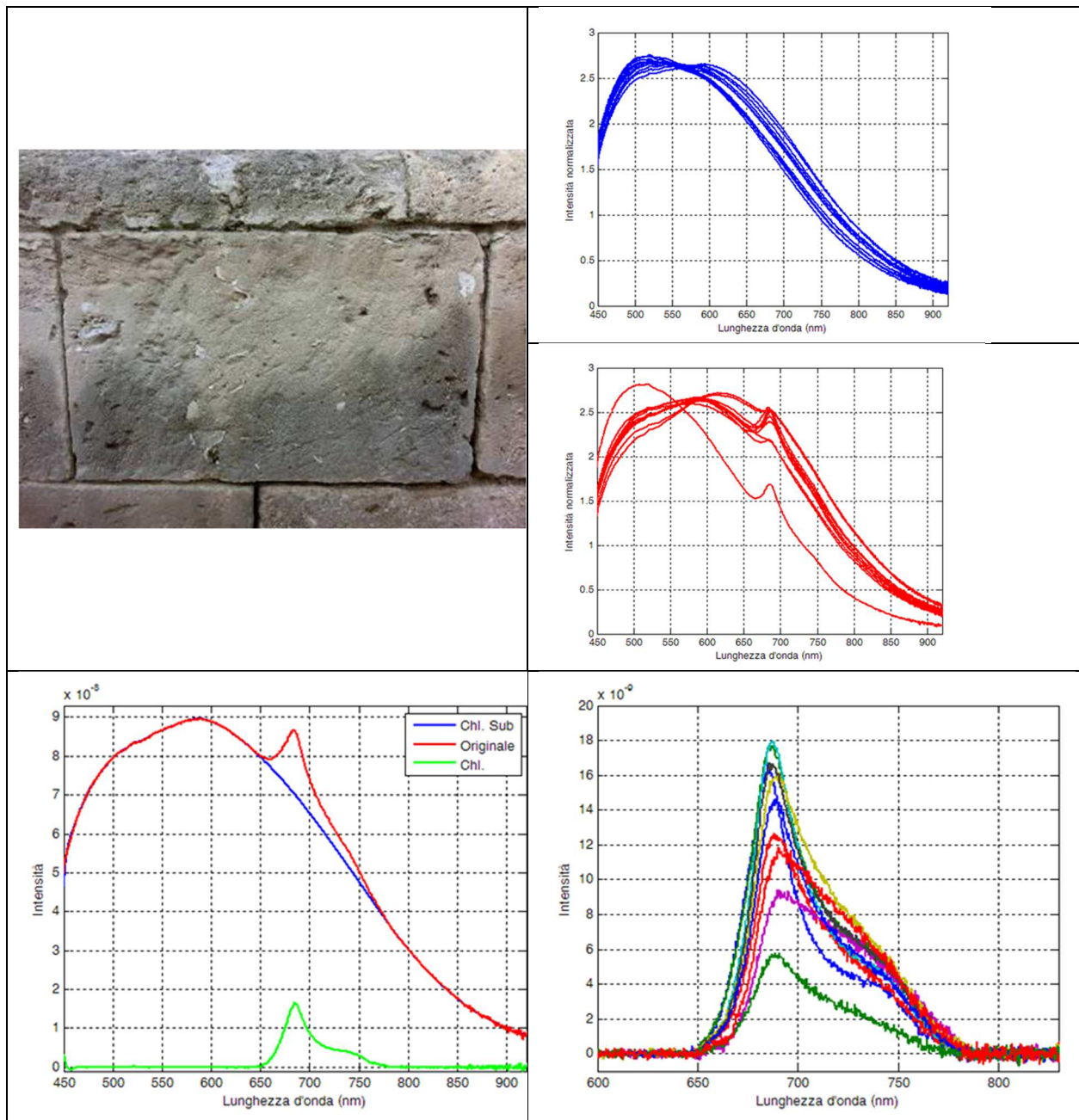
349

350 **3.1 Characterisation of the decay phenomena**

351

352 **3.1.1 LIF investigations**

353 The LIF measurements were mainly performed on selected ashlar of southern wall and from the
 354 façade of the Cathedral, in particular those characterised by dark and clear areas (Figure 4).
 355
 356



357 Figure 4. LIF analysis of the ashlar of the southern wall: (a) Photographic image of one of the examined ashlar featuring
 358 the characteristic dark patina. (b) LIF spectra acquired in various spots of the ashlar, both in the upper and clear part of
 359 the ashlar (red lines) and in the lower and dark part of the ashlar (blue lines). (c) Procedure applied to the acquired LIF
 360 spectra (red line) in order to separate the fluorescence contribution of chlorophyll (green line) from that of the stone
 361 substrate (blue line).
 362 (d) Fluorescence of chlorophyll retrieved from the LIF spectra acquired in various spots of the dark area. All the LIF
 363 spectra were normalised in intensity to their standard deviation. (For interpretation of the references to colour in this
 364 figure legend, the reader is referred to the web version of this article.)
 365

366 Typically, the measurements have been carried out on both the upper (clearer) and lower (darker) part
 367 of the ashlar (Figure 4). The spectra were characterized by the presence of two main contributions
 368 of fluorescence, in a variable ratio, describable as two broad bands centred at about 510 nm and 610
 369 nm. In these spectra the presence of the typical fluorescence peaks of photosynthetic pigments such

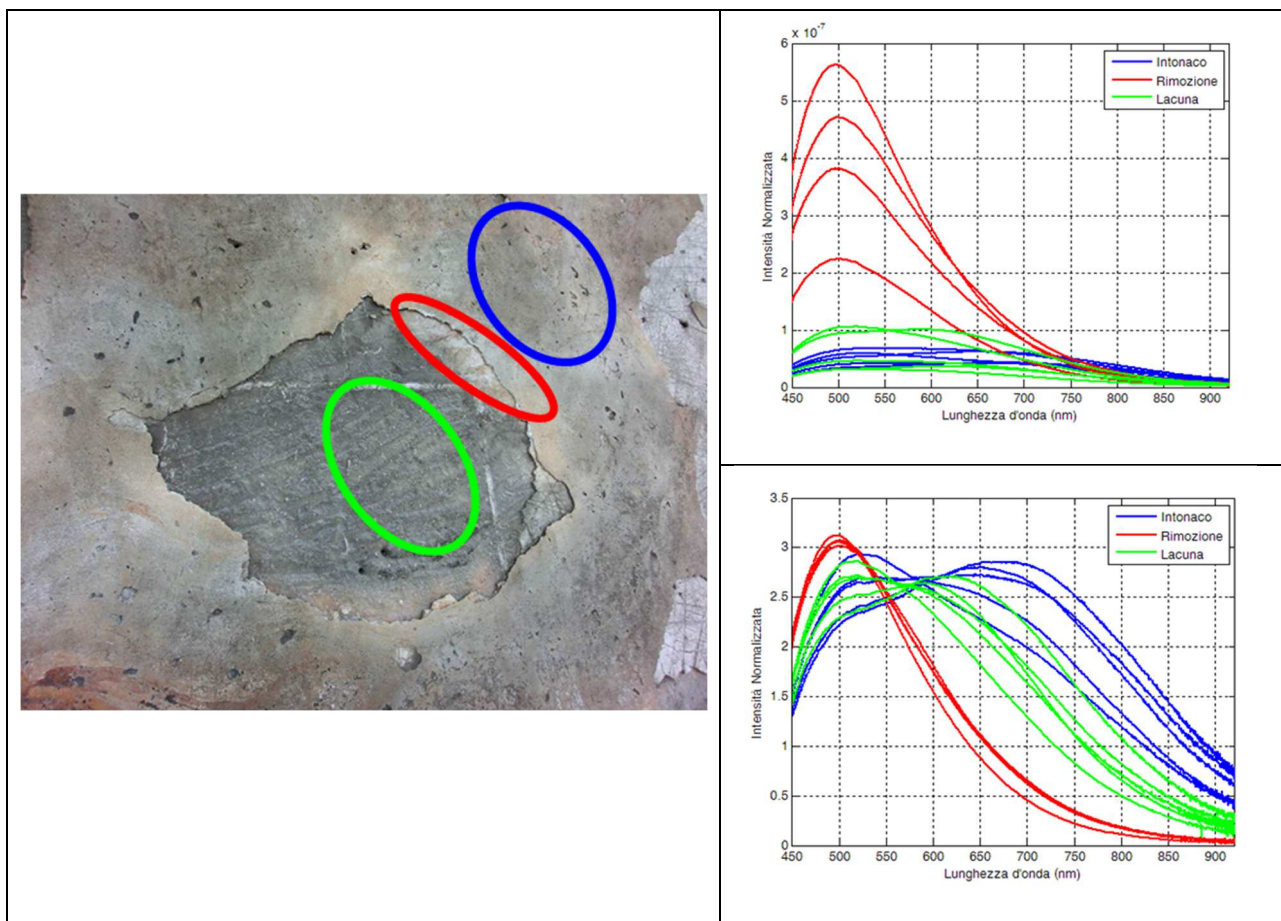
370 as chlorophyll could not be detected. The spectra measured on the upper, clearer, part of the ashlar
371 was characterized by a spectral distribution of the substrate similar to the one detected in the darkest
372 part (broad bands centred at about 510 nm and 610 nm). In these spectra, however, it is present the
373 typical fluorescence spectrum of chlorophyll that is characterized by the typical peak signal centred
374 at about 685 nm and by a spectral shoulder of lesser intensity at about 740 nm. In order to better
375 highlight the typical chlorophyll fluorescence signal, the measured spectra have been further
376 elaborated. On the basis of measurements made in the surface areas not subject to the presence of
377 biological patinas, it is possible to observe that in the spectral range of interest, between about 640
378 nm and 800 nm, there are no particular structures in the fluorescence signal. The spectra were
379 processed, by means of interpolation and reconstruction procedures, so as to estimate the spectral
380 distribution of fluorescence due to chlorophyll. In Figure 4a is shown an example of application of
381 this processing technique. In red it is shown as actually measured fluorescence spectrum that is
382 characterized by the presence of the peak of chlorophyll fluorescence. In blue it is shown the result
383 of the interpolation procedure allowing to estimate the spectrum without the chlorophyll contribution.
384 In green it is shown the fluorescence signal related to chlorophyll clearly highlighting the main
385 contributions at 685 nm and 740 nm. Figure 4b shows the chlorophyll fluorescence spectra obtained
386 by applying this procedure to the spectra acquired on the lower part of the ashlar.

387 These fluorescence signals suggest the presence of a phototrophic biological patina. We have to notice
388 that it was possible to detect the presence of phototrophic patinas exclusively on the upper and clearer
389 part of the ashlar. In order to verify the possible presence of phototrophic organisms in detectable
390 concentration also in the lower and darker part of the ashlar, other fluorescence measurements were
391 carried out after the execution of some mechanical procedures capable to put in evidence the eventual
392 presence of a biological patina that could be inactive and/or not located on the very surface of the
393 ashlar. The applied procedures consisted, in sequence, in the mechanical removal of the very first
394 superficial layer of the dark patina and in moistening with water. Also after this procedure, it was not
395 possible to detect the presence of chlorophyll by means of its fluorescence signal. In some case further
396 test measurements were carried out on the darkest part of the ashlar to verify the lack of the
397 chlorophyll fluorescence signal, determining the presence of the fluorescence signal of such a
398 pigment only in correspondence of alveolus with a diameter of between 4 and 6 mm. Furthermore,
399 the spectral distribution of fluorescence associated to the stone substrate inside the alveolus is
400 distinctly different from that of the surrounding area.

401 Some investigations were carried out also on the St. Eustace statue, which was positioned on the
402 façade. The measurements were carried out on the right shoulder of the statue and on a yellowed area
403 of the aedicule where the statue was housed, just close to samples C6 and C7. The spectra acquired
404 on the shoulder show a main fluorescence contribution with a maximum at about 500 nm and a
405 secondary lower intensity contribution in the 700-750 nm spectral region. The spectra acquired on
406 the aedicule area show a very different spectral distribution, very broad and unstructured, with a
407 maximum between 590 nm and 650 nm.

408 A plastered portion of the façade was analysed too (Figure 5). The surveyed area includes the
409 plastered surface (circled in blue), a portion of stone ashlar from which the plaster was mechanically
410 detached immediately before the measurements (circled in red), and an area in the major plaster gap
411 caused in the past for a plaster detachment (circled in green).

412
413

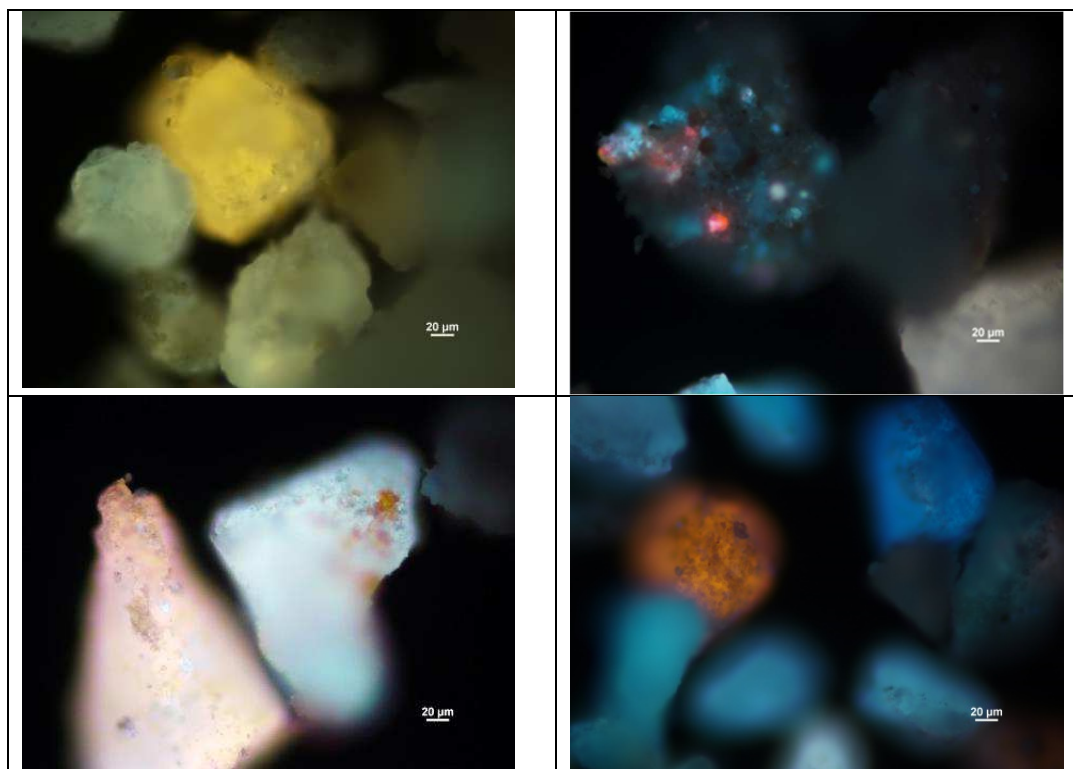


414 Figure 5. LIF measurements on a plastered area of the cathedral's façade. (a) Photographic image of the examined area:
 415 three areas are highlighted in the photo: a plastered area (Area A), an area where the plaster was deliberately detached
 416 mechanically (Area B), and an area corresponding to a former gap in the plaster (Area C).
 417 (b) LIF spectra measured in the three different areas. (c) LIF spectra measured in the three different areas and normalised
 418 in intensity to the relative standard deviation.
 419

420 Figure 6 shows the fluorescence spectra acquired on the three different areas. By comparing the
 421 intensities and spectral distributions of these spectra, it is apparent that the surface exposed because
 422 of the removal of the plaster is characterized by a fluorescence efficiency significantly greater than
 423 both the plastered one and that measured in the area with a lack of plaster caused in the past, as shown
 424 by the spectral distribution. The spectra of the 'old' gap showed a spectral distribution substantially
 425 similar to that observed on the darker areas of other ashlar being characterized by two main
 426 fluorescence contributions at about 500-510 nm and 600-610 nm. The spectra acquired in the area in
 427 which the plaster was manually removed are instead remarkably similar to those acquired on the stone
 428 specimen not treated. This points out that the layer of plaster had in some way protected the stone
 429 from external agents, natural and / or artificial, that caused browning of extended surfaces of the outer
 430 surface of the Cathedral.
 431

432 3.1.2 Biological investigations

433 The powder samples, observed with an optical microscope in epifluorescence showed red
 434 fluorescence due to the chlorophyll of photoautotrophs, while the yellow, orange or blue fluorescence
 435 could be attributed to the presence of other not identified organic products (Figure 6).
 436
 437



438 Figure 6. Autofluorescence examples of the powder samples B1 (above, left), B2 (above, right), B3 (bottom, left) and
 439 B4 (bottom, right).
 440

441 The sample B4 had a lower microbial contamination with respect to the other samples with a greater
 442 biodiversity, especially for the sample B3 (Table 3). The fungal strain *Alternaria* sp. was present
 443 almost all the samples, except B4.
 444

445 **Table 3**

446 The microbial count/presence observed on the three nutrient media; CFU (colony forming units): +/- = scarce, +=
 447 present, ++ = frequent, +++ = abundant.
 448

Media/ samples	Microbial count (CFU/100 mg)			
	B1	B2	B3	B4
PDA (fungal)	1 fungal	2 fungal	3 fungal	1 fungal
PCA (fungal and bacterial)	2 fungal 41 bacterial	1 fungal 37 bacterial	5 fungal 52 bacterial	0 fungal 1 bacterial
BG _{11M} (phototrophs)	++	+++	+++	+/-

449 In the nutrient media used for the development of phototrophic microorganisms, the coccoid
 450 cyanobacteria of the family of *Xenococcaceae*, with spherical mucilaginous colonies was dominant
 451 in all the samples, except for B4 where the presence of phototrophs was insignificant. Other than
 452 cyanobacteria were detected, in the heterotrophic nutrient media, light and deep pink pigmented
 453 bacteria (cocci and rod-shaped), mostly in samples B1, B1 and B3. Some of these bacterial colonies
 454 have an autofluorescence: pink in sample B1 and yellow in sample B2.
 455
 456
 457

458 3.1.3 Chemical and mineralogical investigations

459 *Optical Microscopy*
 460

461 On the basis of observations in transmission mode, the plaster is constituted by an air hardening calcic
 462 lime binder with a homogeneous aspect and a micritic texture. The binder/aggregate ratio is 2:1. The
 463 grain size of the aggregate is bimodal (250-350 mm and 700-800 mm) and the shape of the grains is
 464 from sub-angular to sub rounded. Its composition is characterized by fragments of rock (i.e. Matera
 465 stone), fossiliferous remains and micrite limestone. The porosity is due to the shrinkage cracks.
 466 Regarding to C2 and C3 samples, observed in reflection mode, were interested by a biological
 467 colonization giving a red fluorescence under UV light, due to chlorophyll. C6 sample was observed
 468 in stratigraphy: it is possible to distinguish an alteration superficial layer (about 200 μm thickness)
 469 and a layer constituted by the sound carbonatic stone. Biological colonization was not identified.

470
471
472

473 *X-Ray Diffraction*

474 XRD analyses revealed the presence of whewellite ($\text{CaC}_2\text{O}_4 \cdot \text{H}_2\text{O}$, calcium oxalate monohydrate) in
 475 the samples coming from the facade, with the exception of the plaster C4. Gypsum was detected in
 476 C1 (from southern wall) and in C6 and C7 (from façade). Calcite and quartz are present in all analyzed
 477 samples (Table 4).

478
479
480
481

Table 4

Results of FTIR and XRD analysis of the samples

Sample label	Composition	
C1	calcite, gypsum, alkaline nitrate, silicates, traces of quartz and organic compounds	
C2	calcite, quartz, alkaline nitrate, silicates, traces of clay minerals and organic compounds	
C3	calcite, quartz, alkaline nitrate, silicates, organic compounds	
C4	plaster	calcite, traces of quartz
	external layer	calcite, whewellite, traces of organic compounds
	inner layer	calcite, gypsum, traces of organic compounds
C5	calcite, gypsum, silicates, traces of whewellite and quartz	
C6	bulk	calcite, gypsum, whewellite, traces of quartz
	external layer	gypsum, whewellite, traces of organic compounds
C7	calcite, gypsum, whewellite, silicates	
OG	calcite, quartz, whewellite, traces of goethite	

482

483 *Ionic Chromatography*

484 All samples coming from Southern Wall (samples C1, C2 and C3) were analyzed by means of ionic
 485 chromatography: samples C1 and C2 contain analogous amounts of chloride (Cl^-), nitrates (NO_3^-) and
 486 sodium (Na^+). The amounts of such ions, instead, are lower in sample C3. Sulfates (SO_4^{2-}) are relevant
 487 only in sample C1. Finally, decreasing amounts of potassium (K^+) and calcium (Ca^{2+}) ions are
 488 revealed passing from sample C1 to C2 and to C3. These results suggest the presence of gypsum in
 489 sample C1, coming from blackened area, and of soluble salts (probably sodium and potassium nitrate
 490 and chloride) in samples C1 and C2, coming from areas where the surface is evidently contaminated
 491 by external agent, more than C3.

492 Sample C5 contains low amount of chloride, sodium and potassium, whereas nitrates, sulfates,
 493 calcium and magnesium are present in high amount. Stone powder is so contaminated by gypsum and
 494 soluble salts (presumably calcium and magnesium nitrate and/or organic nitrates).

495 Sample C6 on the contrary contains sodium, nitrates and sulfates in big amounts. Chloride, potassium
 496 and calcium are present in quite significant amount, too. Gypsum and soluble salts (particularly
 497 nitrates, presumably calcium and/or organic ones) are present in this powder too.

498

499 *Infrared Spectroscopy*

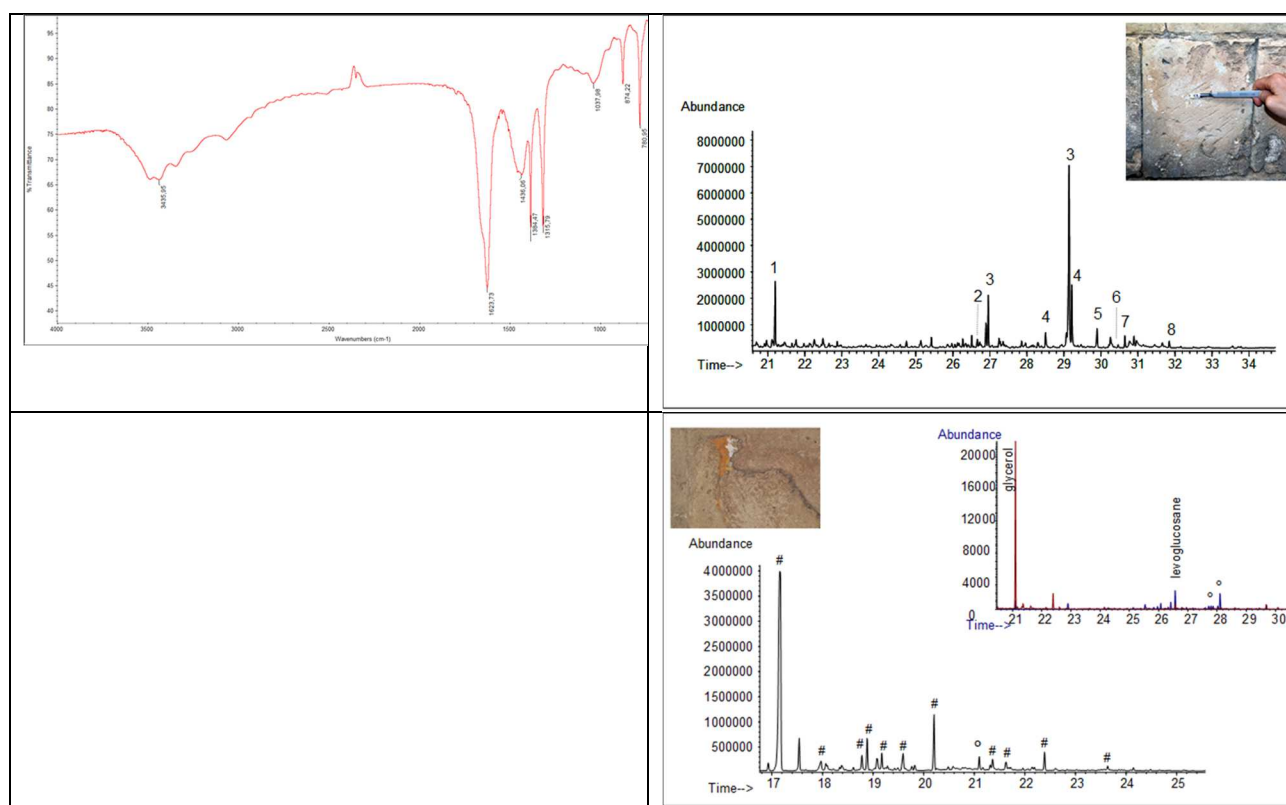
500 FTIR spectra proved very effective in identifying the inorganic component of samples (Table 4).

501 In all the samples the presence of calcium carbonate, in the mineralogical form of calcite, was
 502 suggested by an asymmetric C=O stretching band around 1420 cm^{-1} and by the absorbance at 873
 503 (out-of-plane bending vibration) and 712 cm^{-1} (in-plane bending vibration) [24]. Alkaline nitrate and
 504 silicates were present as well, as shown by the absorbance at 1384 and for the Si-O stretching band
 505 at 1033 cm^{-1} respectively [25].

506 The spectra of samples C1, C5 and C7 present the characteristic sharp peaks of gypsum (CaSO_4
 507 $2\text{H}_2\text{O}$), of hydroxyl stretching bands (3545 and 3408 cm^{-1}) and bending vibrations (1689 and 1622
 508 cm^{-1}), for the S-O asymmetric stretching modes at 1145 and 1116 cm^{-1} , and bending mode at 669 cm^{-1}
 509 $^{-1}$ [24]. Organic matter was found as traces almost in all the samples, with peaks around 2982 and
 510 2875 cm^{-1} , which could be ascribed to CH signals, although FTIR analysis cannot be diagnostic
 511 without the support of more sensitive techniques.

512 The three layers which form sample C4 show the signals of calcite and of traces of organic matter
 513 mentioned before. The features determined in the spectra of the external layer suggest the presence
 514 of calcium oxalate monohydrate mineralogical phase, that is whewellite ($\text{CaC}_2\text{O}_4 \cdot \text{H}_2\text{O}$) (Figure 7).
 515 The identification occurred due to the presence of very specific bands at 3487 , 3435 , 3341 and 3068
 516 (OH stretching bands), 1623 and 1315 (CO stretching vibration), 780 and 674 cm^{-1} (OCO bending
 517 vibrations), which are shown in Figure 13 [26]. The inner layer contains gypsum, as shown by the
 518 typical peaks, which have already been discussed. The same absorbance signals of whewellite were
 519 recognized in the spectra of samples C5 and C7.

520 The external layer of sample C6 is composed by gypsum, whewellite and organic compounds, whose
 521 pattern of peaks might suggest a proteinaceous substance (2962 , 2928 , 2873 , 1508 , 1243 cm^{-1}).
 522



523 Figure 7. Transmission FTIR spectrum of the external layer of sample C4 (left), showing the presence of whewellite
 524 (3487 , 3435 , 3341 , 3068 , 1623 , 1315 , 780 , and 674 cm^{-1}), calcite (1436 , 874 , and 712 cm^{-1}), alkaline nitrates (1384 cm^{-1}),
 525 traces of organic substances (2870 - 2980 cm^{-1}). Pyrogram of sample C3 (right, above), with the most significant
 526 compounds identified: 1: glycerol, 2: levoglucosane, 3: arabinitol, 4: ribitol, 5: hexadecanenitrile, 6: mannitol, 7: palmitic
 527 acid, 8: octadecanenitrile, 9: inositol. Pyrogram of sample OG (right, bottom), with marked the siloxane compounds (#)
 528 together with the markers of a saccharide source (glycerol, levoglucosane and two unknown markers).
 529

530 Pyrolysis Gas Chromatography Mass Spectrometry (Py-GC-MS)

531 The pyrolysis performed on the sample with derivatisation reaction *in situ* [11] allowed the
 532 characterisation of the origin of the organic materials in the thick crust and patina of the façade.
 533 All the samples analyzed presented a variable content of protein. The markers hexadecanenitrile and
 534 octadecanenitrile of egg are shown in the pyrogram of sample C3, reported in Figure 7 as an example.
 535 Particularly interesting are the results obtained from the samples collected from the ashlar which has
 536 been investigated by means of LIF techniques in three different areas (samples C1, C2, and C3). The
 537 analyses highlighted the presence of saccharide material in the clear part of the ashlar (samples C2
 538 and C3) but not in the darkest one (sample C1). In Figure 7 also the markers of saccharide material
 539 are evidenced (glycerol, levoglucosane, arabinitol, ribitol, mannitol, inositol). Most likely, this
 540 material is to be ascribable to the presence of plant cells, as evidenced by the finding of chlorophyll
 541 by the LIF *on-site* investigation. Considering that the saccharide material is absent in the black part
 542 (sample C1), and that sulfates are more abundant in the black area, we can hypothesize that they
 543 inhibit the growth of chlorophylls. The formation of calcium oxalate is possibly originated by the
 544 presence of the proteinaceous material [27–29] which has been probably applied in a *beverone* with
 545 conservation purpose. In fact, being the egg most abundant in the blacker area, we can explain the
 546 presence of darker and thick crust on the bottom of the cathedral walls, with an easier accessibility
 547 for such conservation treatment during the time. Natural resins, waxes or siccative oil are absent.
 548 Finally, the analysis of sample OG (Figure 7), supposed to be an ochre mortar applied by the restorers,
 549 suggested to be a protective siloxane based for masonry. In Figure 7 are reported all the siloxane
 550 compounds identified, together with the markers of a trace of saccharide material.

551
552

553 3.2 Cleaning and protection tests

554

555 3.2.1 Assessment on *ex situ* laboratory tests

556

557 The preliminary laboratory treatments have been applied and tested on ancient noble surface tuff
 558 stone of the Cathedral, with UV light at 254 nm for 72 hours, or without exposition (at 24 hours), as
 559 previously described. The ΔE^* values measured on ancient tuff stone, after treatments by chemical
 560 and biological agents, are summarized in Table 5.

561

562 **Table 5**

563 Colour changes (ΔE^*) measured on *ex situ* tuff stone Matera Cathedral, at 24-72 hours after treatments with chemical or
 564 bio-cleaning agents. Average \pm SD for 3 points obtained in each area.

565

Processes	Treatment	ΔE^*
Chemical	Blank	0.1 ± 0.1
	TiO ₂	2.2 ± 0.3
	TiO ₂ , + UV	3.7 ± 0.4
	UV	0.1 ± 0.2
	H ₂ O ₂	3.4 ± 0.2
	H ₂ O ₂ + UV	4.9 ± 0.4
	Oxone	4.2 ± 0.5
Biological	Laponite gel	2.2 ± 0.4
	Laponite biogel	3.9 ± 0.3

566

567 The colorimetric measurements on the tuff stone showed that the most effective chemical treatments
 568 were H₂O₂ + UV, Oxone and TiO₂ + UV, respectively. However, the tuff area processed with Oxone
 569 resulted, at some points, ruined, so we discarded this oxidant.

570 We noted that only UV radiation had no effect as compared to the control (blank). Moreover, area
 571 treated with TiO₂ appeared “coated” with white pigment; it was washed by deionized water, but the
 572 band remained white. On the contrary, when tuff area was processed with H₂O₂, the brownish

573 alteration was bleached in all surface, raising the cleaning effect when H₂O₂ was combined with UV
 574 exposition (72 h). H₂O₂ is a green and environmental friendly reagent because the only by-products
 575 are water and molecular oxygen; furthermore, H₂O₂ is not an acidic compound and can be utilized
 576 also on the limestone.

577 The results of the biological treatment were determined at 48 hours, after the soft removal of laponite
 578 gel residues by manual brush, when the stone surface was dried by spontaneous evaporation of water
 579 initially contained in the laponite gel. The results by colorimetric measurements showed the effective
 580 of biocleaning agents when laponite biogel enriched of *P. stutzeri* viable cells was applied for 48 h.
 581

582 3.2.2 *On-site* tests on Matera Cathedral wall

583
 584 The results on the application of chemical (AB57 mixtures-poultice and H₂O₂) and biological
 585 (laponite biogel) treatments onto *on-site* selected areas (Table 6) indicate a good compatibility of all
 586 treatments, where the colorimetric measurements performed on the area tested showed ΔE^* values
 587 over the threshold of 3 units; so, the chromatic changes were more than 3 so visible by the naked eye
 588 and as consequence the treated areas at the end of the treatments (i.e, after AB57 poultice or gel
 589 removal) appear affected by less dark alteration (Figure 8). Moreover, when biogel (laponite +
 590 bacteria) was adopted the chromatic change ΔE^* average values were higher 4.75 ± 1.40 compared
 591 to the 4.1 ± 1.28 of laponite alone, but with no statistical evidence. However, in both cases, wide
 592 range of SD values suggesting that the irregular and not homogeneous surface of tuff stone with large
 593 pits and caves, empty spaces, due to loss of materials, exfoliation and decay of surface material,
 594 greatly affected the final results.

595 In the case of chemical cleaning methods, the chromatic change values between the use of H₂O₂ or
 596 AB57 poultice were higher (ΔE^* of 4.95 and 4.65, respectively) and statistically comparable each
 597 other.

598
 599 **Table 6**
 600 Colour changes (ΔE^*) and Water uptake ($g \pm SD$ results at *on-site* sandstone artwork Matera Cathedral, with chemical or
 601 bio-cleaning agents, measured at 48 h, after application.
 602

Area	Treatments	ΔE^*	Water uptake
1-3	Control/Blank	0.70 ± 0.10	0.6 ± 0.1
4-5, 8-10	AB57 mixtures and poultice	4.65 ± 0.50	3.4 ± 0.3
6	Laponite gel	4.1 ± 1.28	2.5 ± 1.4
7	Laponite biogel	4.75 ± 1.40	2.9 ± 1.9
11	H ₂ O ₂	4.95 ± 0.70	3.0 ± 0.6

603



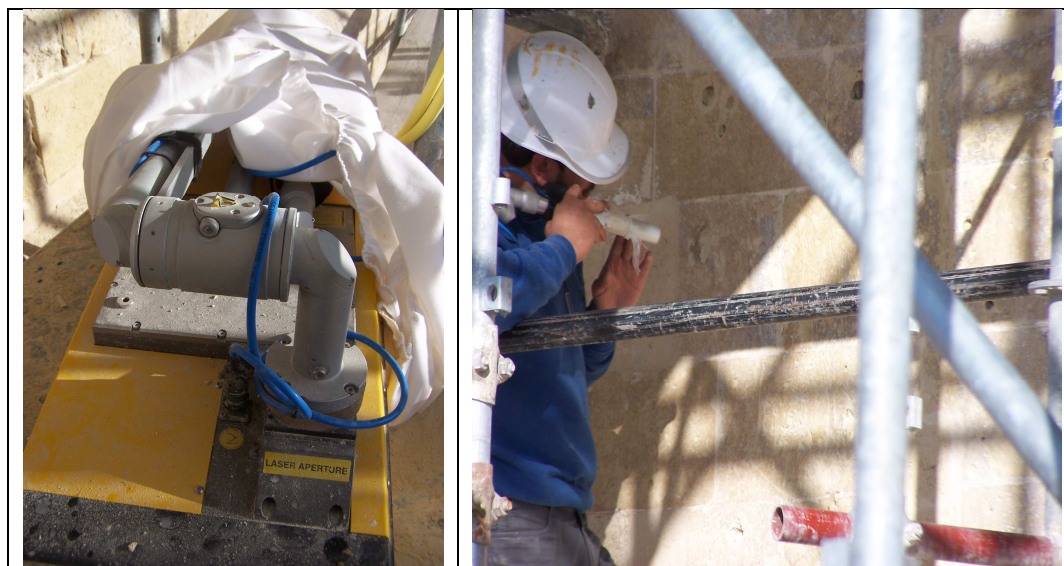
604 Figure 8 *On-site* biocleaning test performed on the lateral tuff wall of Matera Cathedral; laponite biogel bacteria, at 48
605 hours of the bioapplication, before (left) and after (right) the soft biogel removal.
606

607 Moreover, Table 6 shows the values of water uptake (mean+SD in g) by lithoid surface of the left
608 gate near the column, before and after the several tests performed.

609 The calculated data in the treated areas are meaningful different from those made in reference ones
610 (control/blank). In the case of chemical cleaning (AB57) the highest value was obtained with a little
611 range of SD (3.4 + 0.3), demonstrating the high performance of cleaning over all the surface treated.
612 In other cases, the application of laponite gel and laponite biogel bacteria appear to influence at
613 intermediate level the stone substrate in term of water uptake, but with higher DS values, probably
614 due to the irregular of the surface and the presence of *lacunes*. Finally, the values of water uptake
615 after the H₂O₂ treatment appear not meaningful different from those previously cited.
616

617 3.2.3 Physical cleaning by laser technology

618
619 Within restoration activities, which are carried out on works of art of historic and artistic interest,
620 cleaning represents a particularly delicate phase. It is a well-known that the possibility of control,
621 selectivity, preventive evaluation of the effects produced by the intervention, harmlessness both for
622 the restorer and the environment as well as for the work of art, are primary conditions and necessary,
623 for adopting cleaning systems with suitable characteristics for combining the different requirements.
624 The use of laser technology, (a type of physical treatment) has given positive results in this field,
625 adopted especially on limited area on tuff stone surface of Matera Cathedral altered by hard layers of
626 grey-brown crusts that still present even after previously cleaning treatments above cited (Figure 9).
627 As consequence, in fact, the laser cleaning proved to be: i) selective, the shotted beam is absorbed by
628 dirt without affecting the substrata; ii) graduated, the beam power can be selected according to the
629 operator's needs: iii) high quality, when laser was used even on some degraded artworks without the
630 need to pre-consolidate.
631

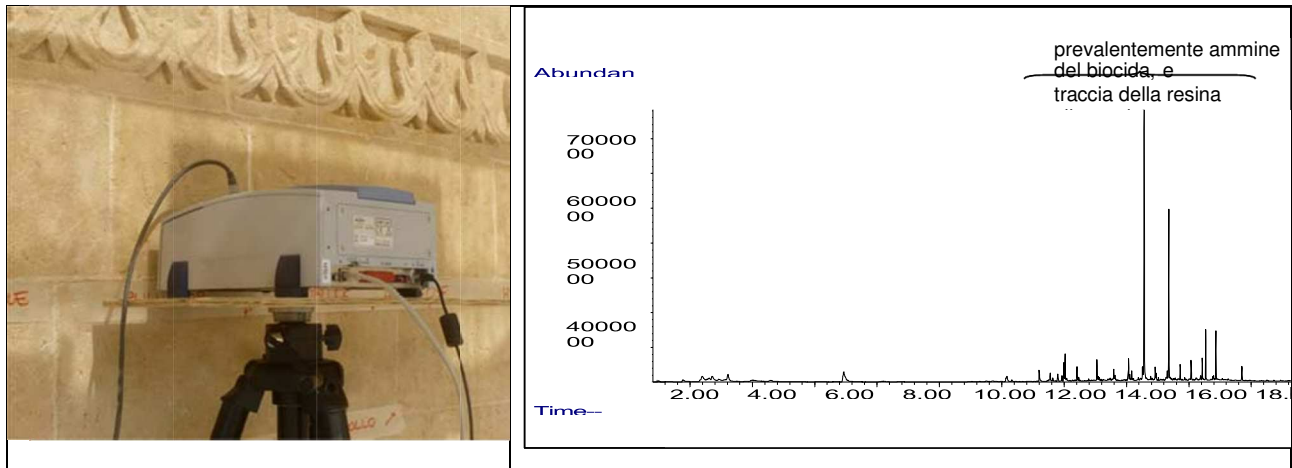


632
633 Figure 9 Micro laser-device and technology adopted on limited area on tuff stone surface of Matera Cathedral
634

635 3.2.4 Protective tests

636
637 Some stone ashlar were treated with ammonium oxalate and ammonium phosphate and treated
638 with the protective agents Pulvistop, Idrobloc and Hydrophase Acqua. The surfaces were
639 monitored by non-invasive FTIR spectroscopy (Figure 10) and Py-GC-MS.

640
641



642
643
644
645

Figure 10 Non-invasive FTIR analysis of an ashlar (left). Pyrogram (right).

646 FTIR results showed the presence of calcite due to the stone substrate. Only in case of the area treated
647 with ammonium oxalate, other weak bands were present. The absorbance at 1318 and 784cm^{-1} were
648 ascribed to calcium oxalate, being the CO stretching and OCO bending vibrations respectively [26].
649 When protective agents were used the SiC signal at 1267cm^{-1} was observed, and in case of Pulvistop
650 the absorbance at 1737cm^{-1} due to acrylic resin was evident.

651 Coming to the Py-GC-MS analysis of micro-fragments of the surface after two months since the
652 application of the protective agents, signals of decay products were absent. The residues of agents
653 Idroblock and Hydrophase Acqua on the surface were much less than the biocide (Figure 10). Test
654 on new formulation of Hydrophase Acqua showed the presence of siloxane, suggesting the use of the
655 type tested on-site.

656

657 3.2.5 Water uptake

658 The results obtained to evaluate the water uptake coefficient on the tuff surface of selected area, by
659 the contact sponge method, showed the best results was obtained with *Hydrophase acqua* [water
660 uptake $1.58\text{ mg}/(\text{min}\cdot\text{cm}^2)$], if compared to the other protective agents tested (article in submission)
661 and to the control area [water uptake $90.05\text{ mg}/(\text{min}\cdot\text{cm}^2)$].

662 The methodology adopted implies manual skill and experience to produce a coherent set of data; the
663 variables involved are in fact not only the imposed pressure but also the compression mechanics; the
664 control on the applied pressure allowed reproducible measurements too.

665

666 4. Conclusions

667

668 This study provides a systematic investigation of the Cathedral of Matera by biological and chemical
669 techniques, also non-invasive, which succeeded in identifying the dark alteration of the external walls
670 as calcium oxalate film.

671 Since the first famous occurrence on the Parthenon at the end of 19th century [30], the phenomenon
672 of calcium oxalate films has been frequently observed in the Mediterranean basin on stone materials
673 (mortars, mural paintings and sculptures) and natural stones of various natures, mainly marble and in
674 several climatic conditions. These films, whose color ranges from ochre to black, are very insoluble
675 in water, thus stable and hardly to remove. The issue about the formation processes of these films has
676 involved the scientific communities at the end of the last century [31,32] debating on the biological
677 or chemical origin. According to the former, calcium oxalate comes from the biofilms on the stone

678 surfaces, producing oxalic acid that reacts with calcium carbonate from the substrate or from deposits
679 [33,34]. On the contrary, oxalic acid could originate from the oxidation of natural organic materials,
680 such as oil, egg and milk, applied in the past on the surface [27,28], being past conservation treatment
681 well documented in the literature for various purposes, such as artificial ageing of new architectural
682 elements, protection against the natural decay, maintenance works.

683 The occurrence of calcium oxalate films has been documented until recent years [2,4,35–37]. In the
684 specific case of the Cathedral of Matera, the two mechanisms could actually occur simultaneously on
685 the stone surface, for the presence of biological activity (cyanobacteria, pigmented heterotrophic
686 bacteria, bacilli and cocci type bacteria) and of residues of organic compounds, which seem to
687 indicate that past conservation treatments were applied. In the specific case of sample C4, the
688 sequence of layers might suggest a past conservation work, when the surface degraded to gypsum
689 was covered by a mixture of calcite and organic compounds, that transformed into calcium oxalate.
690 Where the so-called *beverone*-a mixture of natural organic compounds applied on the stone surface
691 in form of thin film-was not applied, the sulfates, more abundant respect to the calcium oxalate,
692 possibly prevented the growth of microorganisms. LIF measurements in fact showed an 'antagonist'
693 behaviour between the presence of phototrophic biodeteriogens and the presence of the dark alteration
694 of the stones: the chlorophyll is present almost exclusively in areas without dark alteration. Therefore
695 the mechanism of formation of calcium oxalate could be exclusively chemical.

696 The analytical campaign was effective to manage and guide the cleaning tests carried out on stone
697 specimens treated with different cleaning methods. The application of AB57, followed by washing
698 with deionized water, was the most effective method. The test with laser Nd: YAG (El.En) was
699 effective too, but it was carried out only on the carved elements because the cleaning time proved to
700 be too long.

701 Coming to the protective agents, the results suggested the use of Hydrophase acqua, that shows the
702 best performance as does not cross-link and does not film, its colour and composition are constant
703 and gives a good water repellency to the surface. Considering the high porosity of the stone, the
704 surface should be treated again in 3-4 years.

705 Our multi-technique approach was useful for the whole conservation work, in particular the removal
706 of the dark alteration. Figure 11 shows the final appearance of the Cathedral, which will be one of
707 symbols of Matera, that was proclaimed Matera the European Capital of Culture for 2019.

708



709 Figure 11 The Cathedral of Matera before (left) and after (right) the conservation work here reported.
 710
 711

712 **ACKNOWLEDGMENTS**
 713

714 The Authors wish to thank Arch. B. Lafratta, Soprintendenza Beni Architettonici e Ambientali della
 715 Basilicata, Italy; Mons. Lionetti, Arcidiocesi di Matera-Irsina; Impresa D'Alessandro Restauri srl;
 716 Grazia De Cesare. The authors would like to dedicate this manuscript to the memory of Mario
 717 Bressan.
 718
 719

720 **REFERENCES**
 721
 722

- 723 [1] AA.VV., Science and Art: A Future for Stone, in: J. Hughes, T. Howind (Eds.), Proc. 13th
 724 Int. Congr. Deterior. Conserv. Stone, University of the West of Scotland, Paisley, 2016: p.
 725 684.
 726 [2] C. Genestar, C. Pons, J.C. Cerro, V. Cerdà, Different decay patterns observed in a
 727 nineteenth-century building (Palma, Spain), Environ. Sci. Pollut. Res. 21 (2014) 8663–8672.
 728 [3] T. Rosado, A. Reis, J. Mirão, A. Candeias, P. Vandenberghe, A.T. Caldeira, Pink! Why not?
 729 On the unusual colour of Évora Cathedral, Int. Biodeterior. Biodegradation. 94 (2014) 121–
 730 127. doi:10.1016/j.ibiod.2014.07.010.
 731 [4] D. Pinna, M. Galeotti, A. Rizzo, Brownish alterations on the marble statues in the church of
 732 Orsanmichele in Florence: what is their origin?, Herit. Sci. 3 (2015) 7. doi:10.1186/s40494-
 733 015-0038-1.
 734 [5] M. Lettieri, M. Masieri, Surface characterization and effectiveness evaluation of anti-graffiti
 735 coatings on highly porous stone materials, Appl. Surf. Sci. 288 (2014) 466–477.

- 736 doi:10.1016/j.apsusc.2013.10.056.
- 737 [6] V. Crupi, G. Galli, M.F. La Russa, F. Longo, G. Maisano, D. Majolino, M. Malagodi, A.
- 738 Pezzino, M. Ricca, B. Rossi, S.A. Ruffolo, V. Venuti, Multi-technique investigation of
- 739 Roman decorated plasters from Villa dei Quintili (Rome, Italy), *Appl. Surf. Sci.* 349 (2015)
- 740 924–930. doi:10.1016/j.apsusc.2015.05.074.
- 741 [7] R.-M. Ion, D. Turcanu-Caruțiu, R.-C. Fierăscu, I. Fierăscu, I.-R. Bunghez, M.-L. Ion, S.
- 742 Teodorescu, G. Vasilievici, V. Rădițoiu, Caosite-hydroxyapatite composition as
- 743 consolidating material for the chalk stone from Basarabi–Murfatlar churches ensemble, *Appl.*
- 744 *Surf. Sci.* 358 (2015) 612–618. doi:10.1016/j.apsusc.2015.08.196.
- 745 [8] M. Ricca, C.M. Belfiore, S.A. Ruffolo, D. Barca, M.A. De Buergo, G.M. Crisci, M.F. La
- 746 Russa, Multi-analytical approach applied to the provenance study of marbles used as
- 747 covering slabs in the archaeological submerged site of Baia (Naples, Italy): The case of the
- 748 “Villa con ingresso a protiro,” *Appl. Surf. Sci.* 357 (2015) 1369–1379.
- 749 doi:10.1016/j.apsusc.2015.10.002.
- 750 [9] G. Alfano, G. Lustrato, C. Belli, E. Zanardini, F. Cappitelli, E. Mello, C. Sorlini, G. Ranalli,
- 751 The bioremoval of nitrate and sulfate alterations on artistic stonework: The case-study of
- 752 Matera Cathedral after six years from the treatment, *Int. Biodeterior. Biodegradation.* 65
- 753 (2011) 1004–1011. doi:10.1016/j.ibiod.2011.07.010.
- 754 [10] A. Lluveras, I. Bonaduce, A. Andreotti, M.P. Colombini, GC/MS analytical procedure for the
- 755 characterization of glycerolipids, natural waxes, terpenoid resins, proteinaceous and
- 756 polysaccharide materials in the same paint microsample avoiding interferences from
- 757 inorganic media, *Anal. Chem.* 82 (2010) 376–386. doi:10.1021/ac902141m.
- 758 [11] S. Orsini, F. Parlanti, I. Bonaduce, Analytical pyrolysis of proteins in samples from artistic
- 759 and archaeological objects, *J. Anal. Appl. Pyrolysis.* 124 (2017) 643–657.
- 760 [12] R. Rippka, J. Deruelles, J.B. Waterbury, M. Herdman, R.Y. Stanier, Generic assignments,
- 761 strain histories and properties of pure cultures of cyanobacteria, *Microbiology.* 111 (1979) 1–
- 762 61.
- 763 [13] G. Ranalli, G. Alfano, C. Belli, G. Lustrato, M.P. Colombini, I. Bonaduce, E. Zanardini, P.
- 764 Abbruscato, F. Cappitelli, C. Sorlini, Biotechnology applied to cultural heritage:
- 765 biorestitution of frescoes using viable bacterial cells and enzymes, *J. Appl. Microbiol.* 98
- 766 (2005) 73–83. doi:10.1111/j.1365-2672.2004.02429.x.
- 767 [14] G. Lustrato, G. Alfano, A. Andreotti, M.P. Colombini, G. Ranalli, Fast biocleaning of
- 768 mediaeval frescoes using viable bacterial cells, *Int. Biodeterior. Biodegradation.* 69 (2012)
- 769 51–61. doi:10.1016/j.ibiod.2011.12.010.
- 770 [15] P. Bosch-Roig, G. Lustrato, E. Zanardini, G. Ranalli, Biocleaning of Cultural Heritage stone
- 771 surfaces and frescoes: which delivery system can be the most appropriate?, *Ann. Microbiol.*
- 772 65 (2015) 1227–1241. doi:10.1007/s13213-014-0938-4.
- 773 [16] M. Bressan, L. Liberatore, N. d’Alessandro, L. Tonucci, C. Belli, G. Ranalli, Improved
- 774 combined chemical and biological treatments of olive oil mill wastewaters, *J. Agric. Food*
- 775 *Chem.* 52 (2004) 1228–1233.
- 776 [17] L. Liberatore, M. Bressan, C. Belli, G. Lustrato, G. Ranalli, Chemical and biological
- 777 combined treatments for the removal of pesticides from wastewaters, *Water, Air, Soil Pollut.*
- 778 223 (2012) 4751–4759. doi:10.1007/s11270-012-1230-5.
- 779 [18] L. Garrel, M. Bonetti, L. Tonucci, N. d’Alessandro, M. Bressan, Photosensitized degradation
- 780 of cyclohexanol by Fe (III) species in alkaline aqueous media, *J. Photochem. Photobiol. A*
- 781 *Chem.* 179 (2006) 193–199.
- 782 [19] P. D’Ambrosio, L. Tonucci, N. d’Alessandro, A. Morvillo, S. Sortino, M. Bressan, Water-
- 783 soluble transition-metal-phthalocyanines as singlet oxygen photosensitizers in ene reactions,
- 784 *Eur. J. Inorg. Chem.* (2011) 503–509.
- 785 [20] L. Tonucci, F. Coccia, M. Bressan, N. d’Alessandro, Mild photocatalysed and catalysed
- 786 green oxidation of lignin: a useful pathway to low-molecular-weight derivatives, *Waste*

- 787 Biomass Valor. 3 (2012) 165–174.
- 788 [21] UNI-EN 15886:2000. Conservation of cultural property - test methods - colour measurement
789 of surfaces, (1994).
- 790 [22] UNI 11432. Beni culturali Materiali lapidei naturali ed artificiali - Misura della capacita di
791 assorbimento di acqua mediante spugna di contatto, (2011) 6.
- 792 [23] P. Tiano, C. Pardini, Valutazione in situ dei trattamenti protettivi per il materiale lapideo:
793 proposta di una nuova semplice metodologia, *Arkos Sci. E Restauro Dell'architettura*. 5
794 (2004) 30–36.
- 795 [24] M.R. Derrick, D. Stulik, J.M. Landry, *Infrared Spectroscopy in Conservation Science*, The
796 Getty Conservation Institute, Los Angeles, 1999.
- 797 [25] M.J. Wilson, *Clay mineralogy: spectroscopic and chemical determinative methods*, Chapman
798 & Hall, London, 1994. <https://books.google.it/books?id=-EVKpdzHQq8C>.
- 799 [26] I. Petrov, B. Šoptrajanov, Infrared spectrum of whewellite, *Spectrochim. Acta Part A Mol.*
800 *Spectrosc.* 31 (1975) 309–316.
- 801 [27] F. Cariati, L. Rampazzi, L. Toniolo, A. Pozzi, Calcium oxalate films on stone surfaces:
802 experimental assessment of the chemical formation, *Stud. Conserv.* 45 (2000) 180–188.
803 doi:10.2307/1506764.
- 804 [28] L. Rampazzi, A. Andreotti, I. Bonaduce, M.P. Colombini, C. Colombo, L. Toniolo,
805 Analytical investigation of calcium oxalate films on marble monuments, *Talanta*. 63 (2004)
806 967–977.
- 807 [29] R. Bugini, C. Corti, L. Folli, L. Rampazzi, Unveiling the Use of Creta in Roman Plasters:
808 Analysis of Clay Wall Paintings From Brixia (Italy), *Archaeometry*. 59 (2017) 84–95.
809 doi:10.1111/arc.12254.
- 810 [30] J. Liebig, Ueber den Thierschit, *Ann. Der Chemie Und Pharm.* 86 (1853) 113–115.
811 doi:10.1002/jlac.18530860110.
- 812 [31] M. Realini, L. Toniolo, eds., *The Oxalate Films in the Conservation of Works of Art*, in:
813 Editeam, 1996. <https://books.google.it/books?id=tmTqAAAACAAJ>.
- 814 [32] A. VV., *International Symposium on the Oxalate Films: Origin and Significance in the*
815 *Conservation of Works of Art*, in: 1989.
816 https://books.google.it/books?id=G4B_AQAACAAJ.
- 817 [33] M. Vendrell-Saz, W.E. Krumbein, C. Urzi, M. Garcia-Vallès, Are patinas of Mediterranean
818 monuments really related to the rock substrate?, in: *8th Int. Congr. Deterior. Conserv. Stone*,
819 Berlin, 30 Sept.-4 Oct. 1996, 1996: pp. 609–624.
- 820 [34] M. Garcia-Vallès, M. Vendrell-Saz, J. Molera, F. Blazquez, Interaction of rock and
821 atmosphere: patinas on Mediterranean monuments, *Environ. Geol.* 36 (1998) 137–149.
- 822 [35] T. Rosado, M. Gil, J. Mirão, A. Candeias, A.T. Caldeira, Oxalate biofilm formation in mural
823 paintings due to microorganisms – A comprehensive study, *Int. Biodeterior. Biodegradation*.
824 85 (2013) 1–7.
- 825 [36] I. Arrizabalaga, O. Gómez-Laserna, J. Aramendia, G. Arana, J.M. Madariaga, Applicability
826 of a Diffuse Reflectance Infrared Fourier Transform handheld spectrometer to perform in situ
827 analyses on Cultural Heritage materials, *Spectrochim. Acta Part A Mol. Biomol. Spectrosc.*
828 129 (2014) 259–267.
- 829 [37] A. Bonazza, C. Natali, N. Ghedini, C. Vaccaro, C. Sabbioni, Oxalate Patinas on Stone
830 Monuments in the Venetian Lagoon: Characterization and Origin, *Int. J. Archit. Herit.* 9
831 (2015) 542–552. doi:10.1080/15583058.2013.837546.
- 832
- 833